Theory and Practice of On-the-fly and Ultra-fast V_T Measurements for NBTI Degradation: Challenges and Opportunities

*A.E. Islam, E. N. Kumar[1], H. Das[1], S. Purawat[1], V. Maheta[1], H. Aono[2], E. Murakami[2], S. Mahapatra[1], and M.A. Alam

*Email: aeislam@purdue.edu, Phone: 317-701-2184, Fax: 765-494-6441

Department of Electrical and Computer Engineering, Purdue University, West Lafayette, IN 47906, USA; [1]Department of EE, IIT Bombay, India; [2]Renesas Technologies, Tokyo, Japan

Abstract

On-the-fly and Ultra-fast V_T are popular characterization techniques for analyzing NBTI degradation. We show that these techniques do not probe the intrinsic NBTI degradation directly and hence require suitable correction. The 'corrected' data allows us to explore the subtlety of relaxation dynamics by various measurements and suggest a theoretical basis for log-t relaxation consistent within R-D framework.

1. Introduction

In recent years, quantitative analysis of NBTI has dictated replacing the classical, delay-contaminated I_D-V_G measurement of threshold-voltage shift (ΔV_T) by two modern techniques – on-the-fly (OTF) method (standard (S-OTF) [1-3] and fast (F-OTF) [4] versions) and ultra-fast V_T (UFV) [5] technique. There is a widely-held perception that these new techniques probe the intrinsic NBTI degradation *directly* and that the raw measurements can be directly mapped to theoretical models for quantitative analysis [2, 5-10] (see the dashed arrows in Fig. 1). OTF and UFV estimates $|\Delta V_T|$ by measuring $|\Delta I_D/I_{D0}|$ @ constant V_G [2,3,6,8,10] and $|\Delta V_G|$ @ constant I_D [5], respectively. In this paper, we suggest that all these modern methods have significant limitations on their own in ΔV_T estimation (e.g., time-zero delay contamination for OTF; mobility and body effect (m-factor) contamination both for OTF, UFV, and $V_{rec}<0$ for no-delay OTF [10]), thus require suitable corrections (Fig. 3-9). We also identify the necessity of considering valence-band electron trapping into interface traps in analyzing NBTI recovery (Fig. 10-13) as measured by UFV with $V_{rec}\geq 0$. In such case, in addition to $|\Delta V_T|$ relaxation by hydrogenated re-passivation of dangling bonds (N_{IT} recovery), neutralization of dangling bonds (denoted by N_e) by electron capture ($Si^+ + e^- \rightarrow Si$) can also give rise to measured $|\Delta V_T|$ recovery. Thus, the perceived inconsistency between fast-transient relaxation experiments and the prediction of the Reaction-Diffusion (R-D) model [5,9] is addressed by appropriate comparison of the dynamics of $|\Delta V_T|$ and ΔN_{IT}.

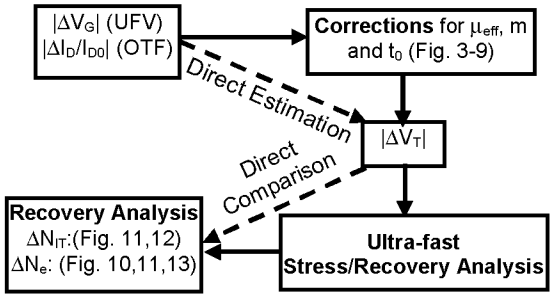

Fig. 1: $|\Delta V_G|$ and $|\Delta I_D/I_{D0}|$ are measured in UFV and OTF techniques and often directly compared to theory (dashed arrows) without correcting for μ_{eff}, m and t_0 or splitting estimated $|\Delta V_T|$ into ΔN_{IT} and ΔN_e components.

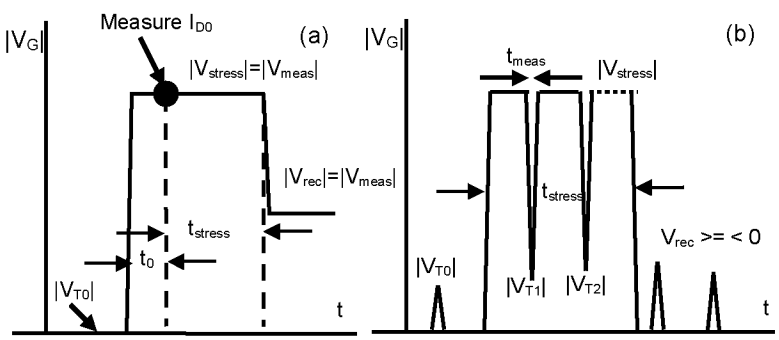

Fig. 2: Timing diagrams for (a) OTF and (b) UFV techniques.

2. NBTI Measurement Challenges

Among the NBTI characterization techniques considered, OTF (Fig. 2a) measures pre-stress V_T (V_{T0}) by I_D-V_G sweep and drain current (I_{D0}) at t_0 (time-zero delay [6, 7], which is ≥ 1ms for S-OTF and ~1μs for F-OTF); then it continuously monitors shift in I_D (ΔI_D) at constant stress-V_G ($V_{stress} = V_{meas}$) for estimating $|\Delta V_T|$ (using $|(V_G-V_{T0})\Delta I_D/I_{D0}|$ [2, 6, 8, 10] or empirical factor [3]). Moreover, recovery-V_G ($V_{rec} = V_{meas}$) for OTF is always above threshold. While in UFV, having t_0=0s (Fig. 2b), $|\Delta V_T|$ (hence, ΔN_{IT}) is directly estimated by measuring $|\Delta V_G|$ at constant I_D ($|V_{meas}| \sim |V_T|$) within $t_{meas} \sim$ 1μs [5], and V_{rec} can be of arbitrary magnitude and polarity. Some of the limitations inherent in such estimation of $|\Delta V_T|$, ΔN_{IT} for OTF and UFV are discussed below.

2.1. Effect of t_0-delay in On-the-fly Techniques

Time-zero delay causes distortion of ΔV_T in short-term stress and contamination of the power-law ($|\Delta V_T| \sim t^n$) time-exponent [$n_{OTF}=n(t-t_0)t^{n-1}/(t^n-t_0^n)$, where n is the time exponent for t_0=0], which can easily be explained using R-D analysis for devices, where NBTI is N_{IT} dominated [4, 10, 11] (Fig. 3a). In spite of increase in n_{OTF} with t_0, all the degradation curves tend to merge at long stress time – indicating the importance of using long-term stress data or appropriately corrected time-exponent for lifetime estimation [8], when t_0>0 in OTF.

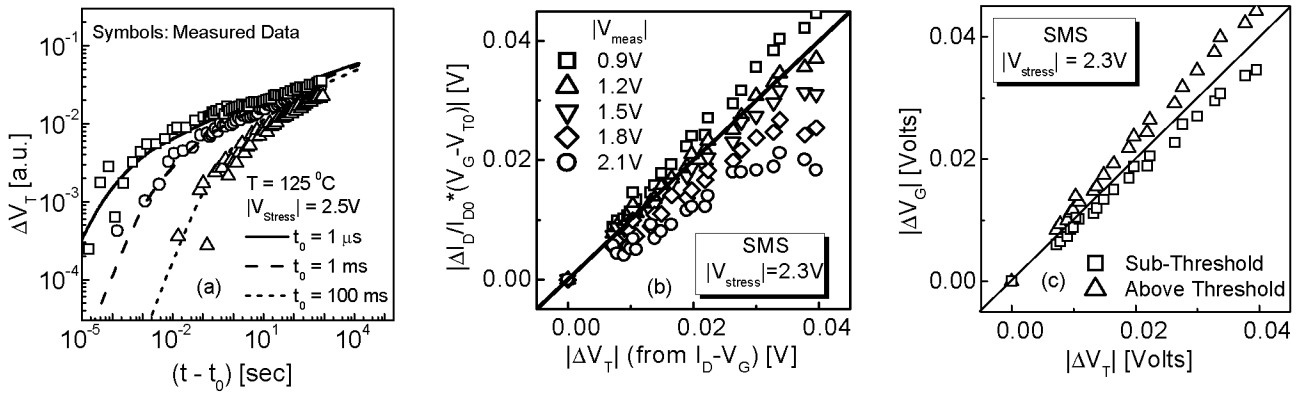

Fig. 3: Measurement Challenges: (a) Effect of t_0-delay for N_{IT}-dominated devices. (b) Classical correction using $|(V_G-V_{T0})|$ factor provides improper $|\Delta V_T|$ estimation in OTF. (c) $|\Delta V_G| \neq |\Delta V_T|$ for UFV, as assumed in [5]; at sub-threshold, $|\Delta V_G|<|\Delta V_T|$ and at slightly above threshold, $|\Delta V_G|>|\Delta V_T|$.

Moreover, once t_0-delay effect is corrected using F-OTF setup [4], low-N_2 samples show good agreement with the predictions from H-H_2 R-D model [7, 12] (Fig. 4). The robust temperature dependence of the initial degradation suggests dominance of N_{IT}-creation over hole-trapping for these devices [4]. It also suggests that *all* fast measurements are not necessarily dominated by hole trapping, as stated in [6]. As initial degradation is small, such observation will not be affected by correction in ΔV_T estimation due to $\Delta\mu_{eff}$ and Δm (discussed later).

2.2. Estimation of ΔV_T

To demonstrate the limitations in classical $|\Delta V_T|$ estimations, we perform a series of stress-measure-stress (SMS) to obtain $I_D(i)$-$V_G(i)$ at various stress times t_i, and thus calculate $|\Delta V_T|$, $|\Delta I_D|$ @ $|V_{meas}|$ and $|\Delta V_G|$ @ I_D. If classical estimates were appropriate for OTF and UFV respectively, plots of $|\Delta V_T|$ vs. $|(V_G-V_{T0})\Delta I_D/I_{D0}|$ (Fig. 3b) and $|\Delta V_T|$ vs. $|\Delta V_G|$ (Fig. 3c) should not have deviated from the straight line, but it does – indicating the necessity of proper $|\Delta V_T|$ estimation.

In order to avoid the fast relaxation phase of NBTI during I_D-V_G sweep, intentional delay is added before each sweep. Moreover, using variable sweep duration (from 0.6-2.7s) both for forward and reverse sweep, similar relations (like Fig. 3b, 3c) are observed in all cases. These prove that Figs. 3b, 3c are not an artifact of extra stress/recovery during I_D-V_G sweep.

2.2.1. Proper ΔV_T Estimation Procedure for OTF

We propose a consistent algorithm for $\Delta I_D/I_{D0}$-ΔV_T mapping for OTF technique (Fig. 5) that rectifies the limitations of previous correction methodologies [3]. SMS is used to monitor change in V_T (by drawing slope at $g_{m,max}$), sub-threshold slope SS (hence, m using SS=2.3mkT/q V/dec) and I_D @ different V_{meas}. Using equations (1) and (2) [13], we can also estimate changes in effective mobility μ_{eff}, μ_0 and θ.

$$I_D = \mu_{eff}C_{ox}W/L\ (V_G-V_T-mV_{DS}/2) \quad ---(1)$$

$$\mu_{eff} = \mu_0 / [1+\theta(V_G-V_T)] \quad ---(2)$$

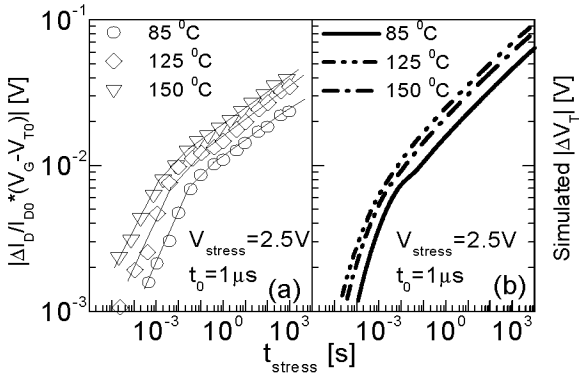

Fig. 4: (a) $|\Delta I_D/I_{D0}(V_G-V_{T0})|$ for devices with negligible hole trapping, which is evident from explicit temperature dependence at early stress phase. (b) Similar temperature dependence is also expected from R-D model (H-H_2) [7, 12].

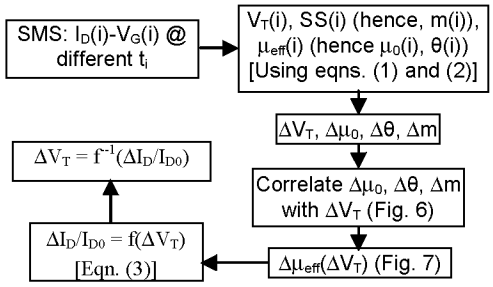

Fig. 5: Algorithm for $|\Delta V_T|$ estimation in OTF from $\Delta I_D/I_{D0}$.

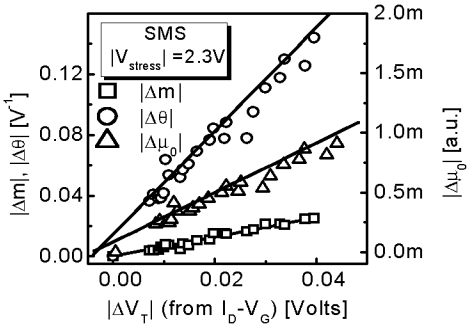

Fig. 6: ($|V_T|$, m) increases and (θ, μ_0) decreases during NBTI degradation. The systematic variation of $|\Delta m|$, $|\Delta\theta|$ and $|\Delta\mu_0|$ with $|\Delta V_T|$, can be used to determine $|\Delta V_T|$ for OTF, as shown in Fig. 8.

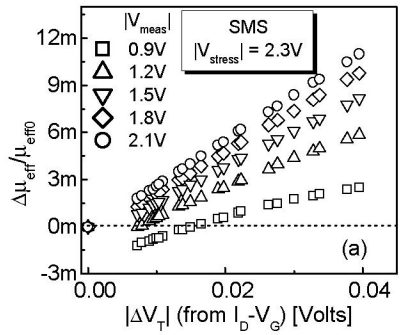

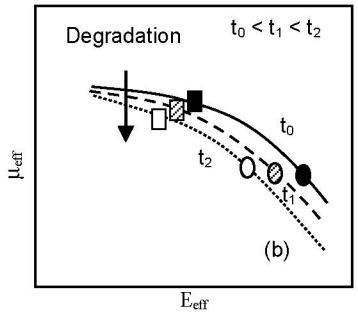

Fig. 7 (a): μ_{eff} above threshold (measurement condition for OTF) decreases (initially for 0.9V) or increases during NBTI. (b) Schematic of μ_{eff} vs. E_{eff} curve. As device degrades, the curve shifts down, changes shape and E_{eff} decreases – resulting $\Delta\mu_{eff}$ to decrease (square) or increase (circle).

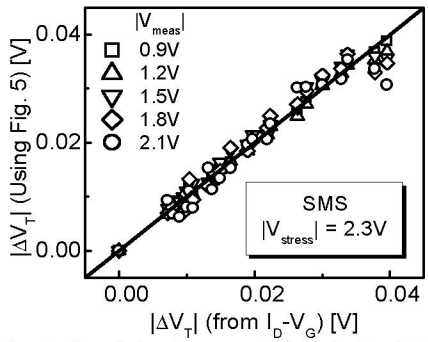

Fig. 8: Correlation between $|\Delta V_T|$ calculated directly from I_D-V_G and indirectly using Fig. 5 is excellent, establishing the validity of the proposed algorithm.

Thus, SMS allows calculation of $\Delta m(\Delta V_T)$, $\Delta\mu_0(\Delta V_T)$, $\Delta\theta(\Delta V_T)$ (Fig. 6) as well as $\Delta\mu_{eff}(\Delta V_T)$ (Fig 7a). The puzzling increase of μ_{eff} with ΔV_T (at high $|V_{meas}|$) is easily explained by realizing that μ_0 degradation due to N_{IT} ($\Delta\mu_0$ [14]) is over-compensated by reduced θ and effective field, E_{eff} (Fig. 7b, circles); this compensation is not present at low $|V_{meas}|$ (Fig. 7b, squares). Finally, equation (3) enables ΔV_T to be estimated as $f^{-1}(\Delta I_D/I_{D0})$. Fig. 8 suggests that the proposed mapping is unique and consistent for all voltages and is an improvement over popular classical estimate, $\Delta V_T \sim\Delta I_D/I_{D0}(V_G-V_{T0})$ (Fig. 3b). Thus, our algorithm works generally for a particular technology (verified using a number of devices), rather than being sample-specific in [3].

$$-|\Delta I_D/I_{D0}| = \Delta\mu_{eff}/\mu_{eff}\ (V_G-V_T-0.5mV_{DS})\ /\ (V_G-V_{T0}-0.5m_0V_{DS}) + \mu_{eff}/\mu_{eff0}\ (-|\Delta V_T|-0.5V_{DS}|\Delta m|)\ /\ (V_G-V_{T0}-0.5m_0V_{DS}) = f(\Delta V_T) \quad \text{--- (3)}$$

2.2.1.1. Time Exponents & Lifetime

The benefit of algorithm in Fig. 5 over classical $|\Delta V_T| \sim|(V_G-V_{T0})\Delta I_D/I_{D0}|$ estimation might lead one to suspect changes in NBTI's power-law behavior and lifetime, reported earlier [2, 8,10,11]. Fig. 9 suggests that while the correction algorithm (Fig. 5) causes negligible change in time-exponents (over classical estimates), the magnitude of $|\Delta V_T|$ – thus estimated t_{life} and V_{safe} [8] – can be significantly different. For higher (lower) $|V_{meas}|$, t_{life} will be over- (under-) estimated and thus will result in a higher (lower) V_{safe}. Hence, after proper correction experimental time-exponents for N_{IT}-dominated devices [4,10,11] will still be ~1/6, thus H-H_2 R-D model [7,12] can be used in analyzing NBTI for such devices.

2.2.2. ΔV_T Estimation for UFV

Fig. 3c indicates that use of $|\Delta V_T| \sim |\Delta V_G|$ in UFV results in over- (if $|V_{meas}| > |V_T|$) or under-estimation (if $|V_{meas}| < |V_T|$) of $|\Delta V_T|$. Similar observation is also reported in [15]. Qualitative explanation of $|\Delta V_T| > |\Delta V_G|$ above threshold can be obtained by differentiating equation (1) at constant I_D or constant E_{eff} (hence μ_{eff} decreases and m increases with degradation), which gives-

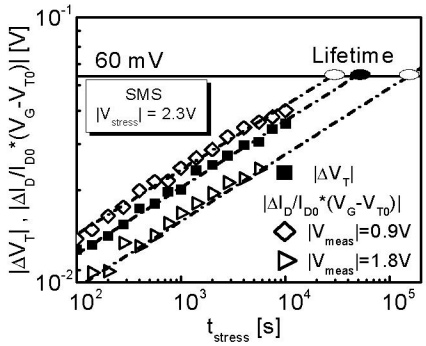

Fig. 9: $\Delta\mu_{eff}$, Δm corrections do not change n; however changes estimated value of OTF-$|\Delta V_T|$, hence changes lifetime @60 mV (solid symbols) compared to classical estimate, $|\Delta I_D/I_{D0}(V_G-V_{T0})|$ (open symbols).

$$\Delta V_G - \Delta V_T = -(\Delta\mu_{eff}/\mu_{eff})(V_G-V_T-0.5mV_D) + 0.5V_D\Delta m \quad \text{---(4)}$$

But lack of accurate I_D expression for the sub-threshold region prohibits analysis similar to Sec. 2.2.1. Thus, although an OTF-comparable correction algorithm can not be proposed for UFV, we suggest caution in interpreting UFV data.

2.3. Estimation of ΔN_{IT}

Estimation of ΔN_{IT} is generally done using $\Delta V_T = q\Delta N_{IT}/C_{ox}$ relationship. Although this equality is proper for OTF (where all donor-type interface traps are charged, as $|V_{meas}|>|V_T|$), the picture is different for UFV. As device switches from stress (Fig. 10a) to recovery, with $V_{rec}\sim0$ (Fig. 10b), part of the donor-type interface traps move below Fermi-level (E_F) and can capture electrons from substrate's valence band. Such electron capture splits interface traps within the band-gap into two parts: empty or positively-charged traps (n_{IT}) and filled or neutral traps (n_e). The time dynamics of these traps are governed by

$$dn_{IT}(E_t)/dt = k_f[n_0-n_{IT}(E_t)] - k_r n_{IT}(E_t)N_H^{(0)} - c_p\exp[-E_t/kT]n_S\ n_{IT}(E_t) + c_p p_S n_e(E_t) \quad \text{--- (5)}$$

$$dn_e(E_t)/dt = - k_r n_e(E_t)N_H^{(0)} + c_p\exp[-E_t/kT]n_S n_{IT}(E_t) - c_p p_S n_e(E_t) \quad \text{--- (6)}$$

where, E_t is trap energy (referred to valence band edge); c_p is capture co-efficient; n_s, p_s are substrate electron and hole

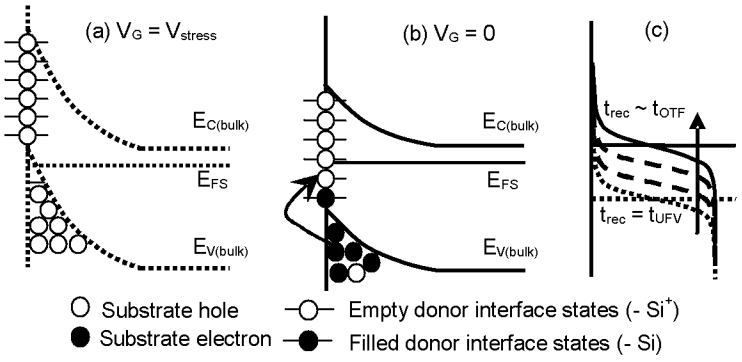

Fig. 10: Band diagram at (a) stress and (b) recovery for UFV. For V_G=V_{stress}, donor type N_{IT} is empty and substrate is filled with holes. For V_G=V_{rec}, fraction of N_{IT} goes below E_F. (c) Energetically suppressed substrate electron capturing makes the trap filling (ΔN_e) a log-t process from $t_{rec} = t_{UFV}$ to ~t_{OTF}.

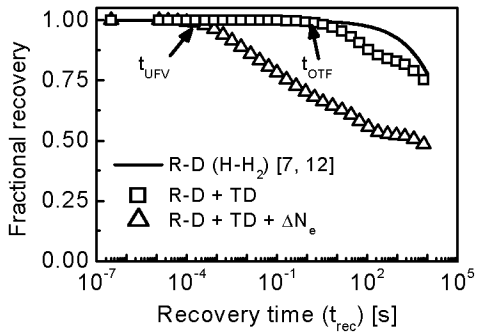

Fig. 11: Presence of ΔN_e (for UFV only) causes ΔV_T recovery (without ΔN_{IT} recovery) to start at t_{UFV}, earlier than predicted by R-D model. In addition, possible existence of transient diffusion will initiate ΔN_{IT} recovery at t_{OTF}.

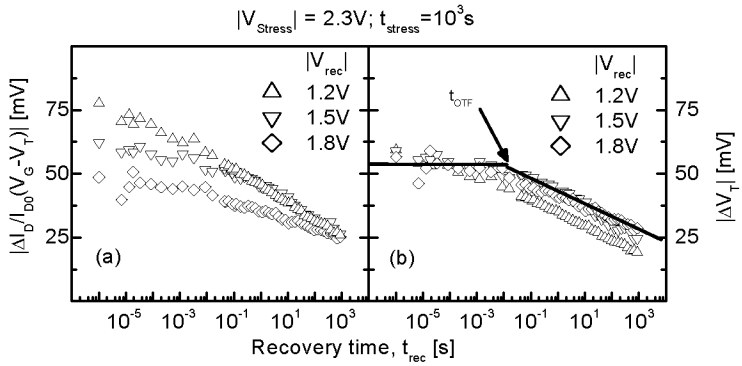

Fig. 12: (a) $|V_G-V_{T0}|$ factor incorrectly estimates different $|\Delta V_T|$ at start of recovery for the same V_{stress}, but different V_{rec}. (b) Estimated $|\Delta V_T|$ using algorithm in Fig. 5 provides consistent results. For OTF, the device is in inversion during recovery, so mechanics of Fig. 10c does not apply and hence recovery starts later compared to UFV (see Fig. 13).

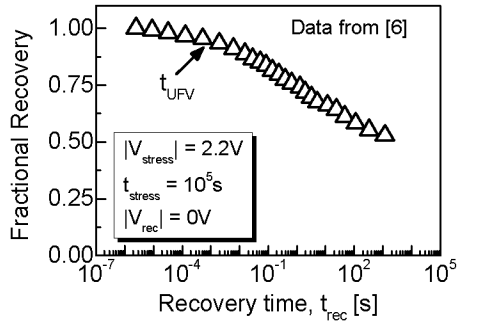

Fig. 13: Uncorrected fractional $|\Delta V_T|$ recovery vs. t_{rec} for UFV. Recovery starts earlier compared to OTF, as electron trapping (Fig. 10c) is expected under this condition.

concentration; k_f and k_r related terms are Si-H bond-breaking and annealing rates, defined in R-D model [7, 12].

Electron trapping causes gradual change of Quasi-Fermi level for traps (Fig. 10c), which *allows fast log-t V_T-relaxation* (starting from t_{UFV} in Fig. 11) *through donor trap neutralization without corresponding re-passivation of N_{IT} by back-diffusing H species* – a slower process predicted by the R-D model [5,9]. For OTF-relaxation, all N_{IT} continues to remain above E_F, thus are unaffected by such trapping (ΔN_e~0 and $\Delta V_T \sim q\Delta N_{IT}/C_{ox}$) – only a faster back-diffusion of H will cause recovery to start at t_{OTF} (Fig. 11). Indeed, since the mobility-corrected recovery for F-OTF (at $|V_{rec}| > 0$, Fig. 12) does not involve electron capture, the relaxation occurs at a later time compared to UFV method (V_{rec}~0, Fig. 13). So NBTI recovery for UFV and OTF has separate dynamics – both consistent within R-D formulation.

Thus, for devices where degradation at long stress time (~10^5 sec in Fig. 13 [5]), is almost certainly dictated by N_{IT} [5, 7, 11], starting of log-t NBTI relaxation from ~µs should not be used to speculate the existence of hole-trapping, as reported in [5,9]. Although, classical R-D mechanism does not support N_{IT}-relaxation from ~µs, it is consisted with ΔV_T relaxation in that time scale through N_{IT} neutralization by valence band electron trapping. Therefore, we emphasize that hole-trapping does not dominate NBTI for all devices, as claimed in [6], but can only explain part of NBTI for certain thick EOT devices having significant interfacial nitrogen [4,10,11].

3. Conclusion

We have critically analyzed the roles of t_0-delay, mobility and body-effect parameter in estimating ΔV_T for both OTF and UFV techniques, used in literature for characterizing NBTI. We present a robust correction scheme for OTF and explore its implications in fast-transient stress and relaxation. Finally, we establish the existence of separate relaxation dynamics for various measurement techniques and suggest a theoretical basis for log-t relaxation within R-D framework.

Acknowledgement: We acknowledge AMAT, TSMC, Renesas, SRC for financial support and NCN for computational resources.

References

[1] Rangan *et al.*, IEDM, p. 341, 2003. [2] Varghese *et al.*, IEDM, p. 684 2005. [3] Parthasarathy *et al.*, IRPS, p. 471, 2006. [4] Kumar *et al.*, IEDM, 2007. [5] Reisinger *et al.*, IRPS, p. 448 2006. [6] Shen *et al.*, IEDM, p. 12.5.1, 2006. [7] Islam *et al.*, *APL*, 90, 083505(8), 2007. [8] Islam *et al.*, IEDM, p. 12.4.1, 2006. [9] Grasser *et al.*, IRPS, p. 268, 2007. [10] Mahapatra *et al.*, IRPS, p. 1, 2007. [11] Islam *et al.*, *TED*, 54(9), p. 2142, 2007. [12] Kufluoglu *et al.*, *TED*, 54(5), p. 1101, 2007. [13] Schroder, Micro. Reliability, 47(6), p. 841, 2007. [14] Krishnan *et al.*, IEDM, p. 349, 2003. [15] Schluender et al., pre-print, IRW '07.